

Pre-print of Polar Science 13 (2017) 23-32; <http://dx.doi.org/10.1016/j.polar.2017.04.001>

1 **Geostatistical analysis and isoscape of ice core derived water stable isotope records in an**
2 **Antarctic macro region**

3 **István Gábor Hatvani^{a,*}, Markus Leuenberger^{b,c}, Balázs Kohán^d, Zoltán Kern^a**

4
5 *^a Institute for Geological and Geochemical Research, Research Center for Astronomy and*
6 *Earth Sciences, MTA, Budaörsi út 45., H-1112 Budapest, Hungary, zoltan.kern@gmail.com*

7 *^b Division of Climate and Environmental Physics, Physics Institute, University of Bern,*
8 *Sidlerstrasse 5, CH-3012, Bern, Switzerland*

9 *^c Oeschger Centre for Climate Change Research, Falkenplatz 16, CH-3012, Bern,*
10 *Switzerland, leuenberger@climate.unibe.ch*

11 *^d Department of Environmental and Landscape Geography, Eötvös Loránd University,*
12 *Budapest, Hungary, balazs.kohan@gmail.com*

13
14 *Corresponding author. Address: Institute for Geological and Geochemical Research,
15 Research Center for Astronomy and Earth Sciences, Hungarian Academy of Sciences, H-1112
16 Budapest, Budaörsi út 45
17 Tel.: +36 70317 97 58; fax: +36 1 31 91738. E-mail: hatvaniig@gmail.com

18
19 **Abstract**

20 Water stable isotopes preserved in ice cores provide essential information about polar
21 precipitation. In the present study, multivariate regression and variogram analyses were
22 conducted on 22 $\delta^2\text{H}$ and 53 $\delta^{18}\text{O}$ records from 60 ice cores covering the second half of the
23 20th century. Taking the multicollinearity of the explanatory variables into account, as also the

24 model's adjusted R^2 and its mean absolute error, longitude, elevation and distance from the
25 coast were found to be the main independent geographical driving factors governing the
26 spatial $\delta^{18}\text{O}$ variability of firm/ice in the chosen Antarctic macro region. After diminishing the
27 effects of these factors, using variography, the weights for interpolation with kriging were
28 obtained and the spatial autocorrelation structure of the dataset was revealed. This indicates
29 an average area of influence with a radius of 350 km. This allows the determination of the
30 areas which are as yet not covered by the spatial variability of the existing network of ice
31 cores. Finally, the regional isoscape was obtained for the study area, and this may be
32 considered the first step towards a geostatistically improved isoscape for Antarctica.

33

34 **Keywords:** $\delta^{18}\text{O}$ & $\delta^2\text{H}$ records, isoscape, polar precipitation, variogram analysis

35

36 **1. Introduction**

37 Due to the increasing interest in the understanding of past global changes, additional
38 and complementary information about past climates is needed. Ice cores play an important
39 role in relation to this issue (EPICA, 2006; NGRIP, 2004; Wolff et al., 2010). For instance,
40 the water stable isotope characteristics stored in them hold crucial information concerning the
41 precipitation they were formed from. The isotopic composition of precipitation, in turn, gives
42 insights into (i) the origin of the water vapor, (ii) the conditions during condensation, and (iii)
43 those during precipitation (Araguás-Araguás et al., 2000; Dansgaard, 1964; Merlivat and
44 Jouzel, 1979). Ice cores can yield information about past climates ranging in time-scale from
45 the seasonal (Hammer, 1989; Kuramoto et al., 2011) up to several hundred millennia (EPICA,
46 2004), and provide relevant indications about the large-scale dynamics of the Earth's climatic

47 system (Jouzel, 2013). By integrating the knowledge gained from studying stable isotopes in
48 ice cores into global circulation models, a more detailed picture can be obtained of the
49 climatic factors driving temporal water isotope variability (Werner and Heimann, 2002).

50 However, dealing with stable isotope data from ice cores in Antarctica is a challenging
51 task, since the spatial availability of cores is sparse and highly variable over the continent
52 (IPICS, 2006; Masson-Delmotte et al., 2008; Steig et al., 2005). Apart from process-based
53 modeling, interpolation is therefore one of the only means available to make estimations
54 between locations for which data are available (Rotschky et al., 2007; Wang et al., 2010).

55 Interpolated maps representing the global distribution of water stable isotopes in
56 precipitation have been developed (Terzer et al., 2013; van der Veer et al., 2009). These,
57 however, do not cover Antarctica. The only product that maps the spatial distribution of stable
58 isotopic composition in Antarctic surface snow (Wang et al., 2010) neglects the shelf areas.
59 Of these regions, the Filchner-Ronne-, Riiser-Larsen and Fimbul ice shelves cover a fair
60 portion of the area investigated in the present study.

61 Isoscapes are predictive models that estimate the local isotopic composition of
62 environmental materials as a function of observed local and/or extralocal environmental
63 variables (Bowen, 2010). The horizontal and vertical resolution of isotope enabled global
64 circulation models (GCMs) are steadily improved (e.g. Werner and Heimann (2002); Xi
65 (2014)), such that isotope enabled GCMs using resolutions previously only attainable in
66 regional models are now available (Sjolte et al., 2011; Werner et al., 2011). In the settings
67 where station based precipitation stable isotope records are available, these are naturally the
68 primary inputs to evaluate the performance of isotope enabled circulation models (Lachniet et
69 al., 2016; Sturm et al., 2005). However, gridded products of precipitation stable isotopes (e.g.
70 isoscapes) can be used as additional benchmarks when observations are missing to assess the

71 global/regional circulation models' effectiveness in replicating observed/interpolated data
72 representing the hydrological cycle and its isotopic counterparts.

73 The aims of this study were (i) to determine the geographic factors driving the stable
74 isotope variability in a chosen Antarctic macro region; (ii) to assess the spatial continuity
75 properties (variograms) of the stable isotope records, an absolute necessity for geostatistical
76 mapping (Herzfeld, 2004), and (iii) to determine the regional isoscape for ice core derived
77 stable isotope records.

78 Variogram analysis was used in the hope that it would reveal those areas insufficiently
79 represented by the current set of ice cores, giving an indication of where their spatial coverage
80 might be increased and reveal the spatial dependence structure of the stable isotope records. In
81 addition, variography is vital for kriging (Cressie, 1990; Oliver and Webster, 2014; van der
82 Veer et al., 2009), an "optimal" interpolation which is then employed in the study to estimate
83 the covariances to the highest degree of accuracy possible before mapping. Consequently, the
84 derived isoscape (Bowen, 2010) will be able to describe the spatial distribution of isotopes in
85 the region in a representative way.

86 Worthy of mention is the fact that the aims of this study are in close agreement with the
87 goals of the International Partnerships in Ice Coring Sciences (IPICS) initiative, since the
88 regional nature of climate and climate forcing requires data from a geographically extensive
89 area. In addition, in order to be able to interpret the water stable isotope records from the past
90 2 ky of ice cores precisely, these have to be supplemented by additional shorter cores for
91 validation (IPICS, 2006).

92

93 **2. Materials and methods**

94 **2.1. Description of the study area and the used dataset**

95 The Antarctic study area (Latitude (LAT): 71°S, 83°S; Longitude (LON): 61°W, 12°E;
96 Fig. 1) covering about 2.6×10^6 km² in the Atlantic sector, was chosen on account of the
97 relatively high abundance of available ice core derived water stable isotope records, and the
98 fact that it disposes of numerous deep ice cores, which have played and continue to play an
99 important role in paleoclimatology. The region is considered to be diverse from both the
100 topographic and glacio-climatologic perspectives, as well (Graf et al., 1994; Oerter et al.,
101 2000; Rotschky et al., 2007), with areas of low elevation (e.g. the Coastal Dronning Maud
102 Land, Ronne Ice Shelf etc.) at sea level, and significantly higher ones (e.g. the Central
103 Dronning Maud Land > ~2500 m a.s.l.). Field observations have shed light on an atypical
104 continental precipitation distribution obtaining in the region, in which the accumulation and
105 mean air temperature decrease with distance from the shoreline and with the increase in
106 elevation (Vaughan et al., 1999). The difference in accumulation between the highly elevated
107 inland regions and the coast may be as great as a factor of six (Graf et al., 1994; Oerter et al.,
108 2000), and vary by up to e.g. $500 \text{ kg m}^{-2} \text{ a}^{-1}$ over a distance of <3 km in certain areas of the
109 Western Dronning Maud Land (Rotschky et al., 2007); for details see Table S1.

110

111 **2.2. Dataset used**

112 The data used were acquired from open access data repositories (NOAA (2014);
113 PANGAEA (2014)) and the corresponding research groups (Divine et al., 2009; Naik et al.,
114 2010). Altogether, an array of 22 $\delta^2\text{H}$ (Fig. S1a & b) and 53 $\delta^{18}\text{O}$ (Fig. S1c & d) records was
115 assembled from 60 ice cores spanning various time intervals. In the compiled ice core derived
116 water isotope database, isotope abundances are expressed as per mil (‰), differences from the
117 V-SMOW standard (Coplen, 1994) using the δ notation, $\delta X = [(R_{\text{sample}}/R_{\text{standard}}) - 1] \times 1000$,
118 where X is ²H or ¹⁸O, R_{sample} is the sample ²H/¹H or ¹⁸O/¹⁶O ratio, and R_{standard} is the ²H/¹H or

119 $^{18}\text{O}/^{16}\text{O}$ ratio of the standard. The longest time interval spanned was almost a millennium
120 (Fig. S1d), while the shortest covered only a couple of years (Fig. S1c).

121 The study was restricted to the period 1970-1988, corresponding to 44 $\delta^{18}\text{O}$, and from
122 1970 to 1989 with 22 $\delta^2\text{H}$ records before pre-processing and filtering. In this way, both the
123 time span and the available number of records were maximized. By choosing the higher
124 number of cores against the longer timescale, the possibility of better signal replication arose,
125 as emphasized e.g by Jones et al. (2009). In addition, there were five ice cores (c5, c7, c9, c11
126 and c13) which only had $\delta^2\text{H}$ records; these were converted to $\delta^{18}\text{O}$ using the regional $\delta^2\text{H}$ -
127 $\delta^{18}\text{O}$ relation established (Fig. S2) based on five neighboring cores with both $\delta^2\text{H}$ and $\delta^{18}\text{O}$
128 records, (for details see SOM). Note that in one special case, the $\delta^{18}\text{O}$ and $\delta^2\text{H}$ records of two
129 cores spaced only 6 km apart, namely, c48 & c49 NM01C82 _04 (B04) and NM02C02_02
130 (FB0202) in Schlosser and Oerter (2002) and Fernandoy et al. (2010) respectively were
131 merged together. These are referenced in the present study under code c62 (Fig. S3). In this
132 way, the total numbers of $\delta^{18}\text{O}$ and $\delta^2\text{H}$ records studied using their 1970-1988 averages were
133 48 and 21 respectively. Reported dating uncertainty of the set of ice cores was $\pm 1\text{yr}$ in both
134 the Dronning Maud Land (Oerter et al., 2000) and the Ronne Ice Shelf (Graf et al., 1999) for
135 the periods closest to the ones assessed in the present study. Therefore, in the case of the
136 $\sim 20\text{yr}$ averages used in the study, dating uncertainty documented above is expected to be
137 negligible.

138 It is generally acknowledged that the isotopic composition of meteoric precipitation is
139 related to geographical position (Dansgaard, 1964), and can be statistically modeled
140 employing geographical parameters (Bowen and Revenaugh, 2003). These global trends can
141 indeed be generalized to the Antarctic continent (e.g. Wang et al., 2009). On a regional scale,
142 however, the set of independent variables to describe isotope variations may change. In order
143 to be able to analyze the spatial autocorrelation and derive an isoscape of the stable isotope

144 records, their dependence on geographical factors has to be determined, as in Lorius and
145 Merlivat (1977) or Smith et al. (2002). For the reasons for this and further details, see Section
146 2.3.

147 Therefore, in order to determine the geographical factors controlling the ice core water
148 isotopes' variability, latitude (LAT), longitude (LON), elevation (ELE), and distance from the
149 coast (D) were considered in this study. LAT & LON were obtained from the original
150 repository files and converted into meters on a polar stereographic projection with reference
151 to the World Geodetic System 1984 ellipsoid. ELE was extracted from the high-resolution
152 Antarctic digital elevation model (DEM) of Liu et al. (1999), while D was calculated using
153 the shortest perpendicular distances between the sample points representing the ice cores and
154 the coast line.

155

156 **2.3. Determination of the geographic factors controlling the water stable isotope** 157 **variability in firn and ice**

158 In order to obtain representative results on the chosen scale from variography, first the
159 effect of the geographical factors controlling the water stable isotopes' variability in fresh
160 and/or metamorphosed snow has to be minimized (Füst and Geiger, 2010; Hohn, 1999). This
161 is because these factors influence the variability of the inspected parameter on a similar and/or
162 larger scale than the phenomena investigated, masking the finer scale pattern, resulting in
163 non-stationarity (Hohn, 1999).

164 The following procedures refer only to the $\delta^{18}\text{O}$ parameter, because after pre-
165 processing, the number of available $\delta^2\text{H}$ records was found to be too low (for details see
166 Section 3.1). In the case of the Antarctic study area, the spatial/geographic dependence of

167 precipitation stable isotope composition is well documented (Lorius and Merlivat, 1977;
168 Masson-Delmotte et al., 2008). In the light of these facts, and following the path indicated by
169 previous studies, multiple regression analysis (Draper and Smith, 1981) was chosen to
170 diminish the influence of topography on such first order factors as e.g. condensation
171 temperature and distillation, leaving the effect of the second order factors such as local air
172 mass trajectories and different moisture sources in the residual field.

173 However, unlike previous studies, multiple factors (e.g. variance inflation, mean
174 absolute error) were taken into account together - as suggested by O'Brien (2007) - to find the
175 best combination of driving parameters.

176

177 **2.4. Variography**

178 **2.4.1. Theoretical background of the semivariogram**

179 The basic function of geostatistics, the variogram, is a tool for describing the spatial
180 autocorrelation structure of the explored variable and to obtain the weights necessary to be
181 able to predict the values of the Antarctic ice core derived $\delta^{18}\text{O}$ annual signal at unsampled
182 locations using kriging techniques (Herzfeld, 2004). The variogram can be described
183 mathematically as follows (Molnár et al., 2010): Let $Z(x)$ and $Z(x+h)$ be the values of a
184 parameter sampled at a planar distance $|h|$ from each other. If samples are taken from the
185 same population (stationarity), and they are in accordance with the intrinsic hypothesis of
186 geostatistics, then the variance (VAR) of the difference of $Z(x)$ and $Z(x+h)$ in a given direction
187 is:

$$188 \text{VAR} [Z(x+h) - Z(x)] = \text{VAR} [Z(x+h)] + \text{VAR} [Z(x)] - 2\text{COV} [Z(x+h), Z(x)] = 2\gamma(h) \quad (1)$$

189 The function $2\times\gamma(h)$ is called the parameter's variogram, while $\gamma(h)$ is its semivariogram and

190 COV stands for covariance. The semivariogram may be calculated by the Matheron algorithm
191 (Hohn, 1999; Matheron, 1965):

$$192 \quad \gamma(h) = \frac{1}{2N(h)} \sum_{i=1}^{N(h)} [Z(x_i) - Z(x_i + h)]^2 \quad (2)$$

193 where $N(h)$ is the number of lag- h differences, i.e. $n \times (n-1)/2$ and n corresponds to the number
194 of sites. The most important properties of the function (Fig. 2) are: the value C_0 (“nugget”)
195 which withholds information regarding the error of the sampling; the level at which the
196 variogram stabilizes is the sill (C : partial sill + C_0 : nugget) which is equal to the variance for
197 stationary processes, and the range (a) is the distance within which the samples have an
198 influence on each other (Webster and Oliver, 2008) and outside of which they are quasi-
199 independent (Chilès and Delfiner, 2012). This distance (range) determines the average area of
200 influence surrounding the sample locations, within which the measured values of the variable
201 explored are interconnected. In the case of isotropy (Chilès and Delfiner, 2012), the spatial
202 range equals the radius of the area of influence.

203 If $\gamma(h)$ is a monotonically increasing function (if $h \rightarrow \infty$ then $\gamma(h) \rightarrow \infty$), the parameter
204 is non-stationary (e.g. in Fig. 3). Moreover, if the semivariogram does not have a rising part,
205 the empirical semivariogram’s points will align parallel to the abscissa, giving a nugget-effect
206 type of variogram. In this case, the sampling frequency is insufficient to estimate the range
207 (Hatvani et al., 2014).

208 Empirical semivariograms by themselves are not yet applicable in spatial modeling.
209 They have to be approximated by theoretical functions in order to provide the necessary
210 weights to be used in kriging (Cressie, 1990) for predicting values at unsampled locations
211 (Chilès and Delfiner, 2012; Herzfeld, 2004). However, a thorough discussion of this question
212 is beyond the scope of the present paper.

213 From the technical perspective, the variogram analysis was conducted on the residuals
214 of the best multiple regression model of the stable isotope records, with a maximum lag
215 distance set to 600 km and 11 uniform bins about 55 km wide. For further details, please see
216 section 2.3.

217

218 **2.4.2. Preliminary variography on raw data before minimization of the effect of** 219 **the geographical factors**

220 Empirical semivariograms were derived from the original/raw data for $\delta^{18}\text{O}$ and $\delta^2\text{H}$.
221 Increasing values of γ were observed for both parameters. For $\delta^{18}\text{O}$ a strictly monotonic
222 pattern; while for $\delta^2\text{H}$, two increasing sections were seen: from the smallest lag distance to
223 ~250 km, then from ~370 km onwards (Fig. 3). It should be noted that in the case of $\delta^{18}\text{O}$ no
224 peaks can be seen as a result of the overwhelming masking effect of geographical factors on
225 water stable isotope variability. Such a variogram cannot be used for further evaluation, as
226 explained in Section 2.4.1. Moreover, in the case of $\delta^2\text{H}$, because of the low number of ice
227 cores (Fig. 1b), γ values could have been calculated for only a few pairs at almost all lag
228 distances (Fig. 3b). Thus, $\delta^2\text{H}$ had to be left out of further analyses.

229 As discussed in Section 2.3. geographic factors controlling the water stable isotope
230 variability in firn and ice, and their effect has to be minimized. The previous observations on
231 the particular dataset at hand, therefore, further verify the necessity of the minimization of the
232 determining effect of geographic factors controlling the water stable isotope variability in firn
233 and ice before variography can be commenced.

234

235 **2.5. Isoscape derivation**

236 The procedure of isoscape derivation for the studied Antarctic macro region is based on
237 the methodology used for the global isoscape (Bowen and Wilkinson, 2002) and for an
238 isoscape of an Alpine domain (Kern et al., 2014). The main idea is to:

- 239 (i) create an *initial grid* of the stable isotope variance in the region described by the
240 multiple regression model of the supposedly driving geographic variables (LAT, LON,
241 ELE, D). This step was carried out with the ArcGIS Spatial Analyst Raster Calculator
242 tool;
- 243 (ii) create an interpolated (ordinary point kriging) *residual grid* using the theoretical
244 semivariogram (Section 2.4) fitted on to the residuals of the multivariate regression
245 model; and
- 246 (iii) summarize the corresponding initial (i) and residual (ii) grids to obtain the final map.

247 Both initial and residual grids were generated uniformly at a resolution of 5 km to
248 facilitate grid calculation. All computations were performed using Golden Software Surfer 11,
249 ArcGIS 10, IBM SPSS 20 and GS+ 10. For certain visualizations of the results, a
250 CorelDRAW Graphics Suite X6 and MS Office 2016 were used.

251

252 3. Results

253 3.1. Minimization of the effect of geographical factors on water stable isotope 254 variability

255 Motivated by the variogram results on the raw data and the pioneering works of Lorius
256 and Merlivat (1977) and Masson-Delmotte et al. (2008), the geographical factors controlling
257 $\delta^{18}\text{O}$ variability in the region were determined/modeled. The values of the multivariate
258 geographical models were subtracted from the averages of firn/ice $\delta^{18}\text{O}$ records (raw data). In

259 this way the effects of geographical factors on the averages of firn/ice $\delta^{18}\text{O}$ records for the
260 period 1970-1988 were corrected.

261 Multivariate regression models were computed and compared using independent
262 variables in various combinations of LAT, LON, ELE and D (SOM Table S2). For example,
263 if LON was omitted, adjusted R^2 (R^2_{adj})=0.98; mean absolute error (MAE) equals 0.87, and a
264 higher degree of multicollinearity was observed than in the case when LAT was omitted. In
265 fact, the latter case was found to be the most robust choice ($p < 0.01$) for estimating oxygen
266 isotope variation on geographical parameters, $\delta^{18}\hat{\text{O}}$, (Eq. 3) with an R^2_{adj} =0.98, MAE of 0.95,
267 and an acceptable degree of multicollinearity, which needs to be evaluated in the context of
268 several other factors influencing it (O'Brien, 2007).

269

$$270 \delta^{18}\hat{\text{O}} = -(20.51 \pm 0.57) + (2.64 [\pm 0.57] \times 10^{-6}) \times LON - (5 [\pm 0.27] \times 10^{-3}) \times ELE - \\ 271 (1.9 [\pm 0.12] \times 10^{-5}) \times D \quad (3)$$

272 It should be noted that the uncertainty of the coefficients in the squared brackets is the
273 standard error (SE).

274 The R^2_{adj} =0.98 may imply that only 2% variance remains in the residuals. However, this
275 is just a method specific and insufficient estimate of the real unexplained spatial variance
276 which is definitely larger (Cressie, 1993). Thus, it has to be explored using variography. The
277 classical non-spatial model (multivariate regression in the present paper) is a special,
278 simplified case of a geostatistical model which is more general (Cressie, 1993). The statistical
279 range of the residuals of the multiple regression spans ~5‰, in addition, their map indicate a
280 spatial structure (Fig. 4a). For instance, negative residuals are observed west of the Berkner
281 Island, or close to zero in Dronning Maud Land and positive ones are clustered south of the

282 Ronne Ice Shelf. The two ice cores on Berkner Island (c1 & c2) gave two of the most positive
283 residuals. This may be explained by the elevated location of ice cores c1 & c2. It suggests that
284 the regional isotopic altitude effect might be unsatisfactory (too steep) here. The regional
285 isotopic altitude effect is mainly determined by the less depleted $\delta^{18}\text{O}$ compositions,
286 characterized by the low elevated ice-shelf sites and the more depleted compositions
287 characterized by high elevated central Dronning Maud Land. The explanation for these two
288 positive extremes can be that the hills of the Berkner Island are located right at the edge of the
289 ice shelf, but at a relatively higher latitude. The discrepancy suggest that the main physical
290 parameters (arrival temperature, remaining vapor fraction etc.) have a somewhat different
291 effect on the isotopic Rayleigh process compared to the regional average. The strong local
292 influence clearly lead to deviations and the multiple regression model was unable to follow
293 this microregional pattern (Fig. 4a). Thus, ice cores c1 and c2 were left out during
294 variography, but were included in the spatial interpolation step.

295

296 **3.2. Variography**

297 The empirical semivariogram of the $\delta^{18}\text{O}$ residual was computed with a maximum lag
298 distance set at 600 km, chosen in accordance with the spatial distribution of the cores. The
299 number of cores between 600 and 650 km clearly drops (Fig. S4); as a result, the number of
300 pairs forming the basis of the variogram decreases as well at over ~600 km (Fig. 4b). In
301 addition, with the 55km bins, by keeping the number of pairs relatively even (Fig. 4b) its
302 reliability was ensured. After the empirical variogram was obtained, a best-fit spherical model
303 was determined ($R^2= 0.72$; residual sum of squares was 0.68) following the protocol strongly
304 recommended by Oliver and Webster (2014).

305 It is clear that the theoretical variogram is not of the nugget-effect type (for a
306 description, see Section 2.4). After a rising part, it stabilizes at a point just slightly above the
307 variance after reaching the sill (C_0+C), yielding a roughly 350 km spatial range for the
308 average of the 19 years of $\delta^{18}\text{O}$ data used (Fig. 4b). This variogram was later on used to
309 provide the weights for the residual grid derived with ordinary point kriging (Fig. 4c). The
310 standard deviation of the kriging ranged from 0.45 to 1.48 (Fig. 4d). The fact that the kriged
311 map of the residuals (Fig. 4c) reflected a spatial structure and not random noise, clearly
312 indicates that the multivariate regression model was not able to capture this meaningful
313 portion of the spatial variance structure of the firn/ice $\delta^{18}\text{O}$.

314

315 **3.3. Isoscape derivation for $\delta^{18}\text{O}$**

316 The initial grid was derived employing LON, ELE and D as the main geographical
317 factors driving the $\delta^{18}\text{O}$ variability of firn/ice (Eq 3). The residual grid was modeled using the
318 weights provided by the variogram of the residual $\delta^{18}\text{O}$ (Section 3.2). Afterwards, the initial
319 and residual grids were summed and the regional isoscape of the mean firn/ice $\delta^{18}\text{O}$ was
320 obtained (1970-1988).

321 The values of the residual grid varied by up to 11.8% of the initial grid (Fig. S5),
322 containing a fair portion of the spatial variance of the snow/firn $\delta^{18}\text{O}$. Thus, if the residual
323 grid had not been taken into account, this would have been lost. With the average spatial
324 range, the area of influence can then be plotted and unified for the set of examined ice cores.
325 This union indicates the areas where the spatial model is reliable from the geostatistical point
326 of view (Fig. 5), while the map of the standard error of kriging offers an alternative measure
327 of the accuracy of the derived $\delta^{18}\text{O}$ isoscape (Fig. 4c).

328

329 **4. Discussion**

330 **4.1. Dependence on geographical factors**

331 Since the main aim of the present study was to determine the spatial range using
332 variography, the effect of the regional geographical factors on firn/ice $\delta^{18}\text{O}$ variability had to
333 be minimized. For decades, scientists have been keenly studying the relationship between
334 geographical factors and the stable water isotope composition of surface snow and firn in
335 Antarctica both on a continental and a regional scale, for example Lorius and Merlivat (1977)
336 and the others as may be seen in Table 1.

337 In regional studies, the number of independent variables applied has in general been
338 smaller than in the present case. In certain Antarctic macro regions the set of geographical
339 factors governing the distribution of stable water isotopes has mainly been determined by
340 elevation (Altnau et al., 2015; Smith et al., 2002). It should be emphasized that in the present
341 case LON, ELE & D explained 98% of the variance in the area explored, just as in the work
342 of Altnau et al. (2015), which overlapped with a fair portion of the western part of our studied
343 region.

344 In general the explanatory power of the models in these studies was lower than those
345 used here, and although there were cases when multiple criteria were used to evaluate the
346 models (Wang et al., 2010), this was not the most common practice. Usually R^2 was used (e.g.
347 Altnau et al. (2015); Masson-Delmotte et al. (2008)), and despite its importance (O'Brien,
348 2007), no attention was paid to multicollinearity, unlike in the present study. In addition, the
349 data gathered here were homogeneous, inasmuch as firn/ice core data uniformly averaged for
350 1970-1988 were used. Casual snow samples or averages of hundreds of meters of ice cores
351 were omitted to avoid potential bias towards a short or extraordinarily long time frame. These

352 considerations make the presented approach more reliable for the region than any other
353 previously.

354 A comparison with previous studies partially overlapping in time and/or space on the
355 dependence of these geographical factors led to meaningful results only in the case of
356 elevation. The value of 0.005 ‰ m^{-1} obtained in the present study was of the same order as
357 those in the literature, but was one of the lowest among them even if uncertainty (SE in Eq. 3)
358 is taken into consideration. In particular, for the investigation of areas ranging between the
359 coastline and the East Antarctic Plateau (Altnau et al., 2015; Smith et al., 2002), the
360 coefficient of elevation (0.008 ‰ m^{-1}) was higher than that in the present study. For research
361 conducted on a continental scale, the derived coefficients have been lower (0.007 ‰ m^{-1}
362 Masson-Delmotte et al. (2008) and 0.0068 ‰ m^{-1} (Wang et al., 2010)). Our lower value can
363 be explained by the fact that only a small part of the area investigated here extends onto the
364 East Antarctic Plateau where a steeper elevation effect was observed.

365 The two most outlying model residuals suggested that the multivariate regression
366 applied here was unable accurately to capture the microregional characteristics of the elevated
367 relief of Berkner Island (c1 & c2) rising between the Ronne and Filchner Ice Shelves (Fig. 1).
368 These regional differences lead to the omission of ice cores c1 and c2 from the multiple
369 regression model.

370 On the basis of the results presented here, it may be suspected that on the scale of the
371 investigated region LON, distance from the coast (D) and elevation (ELE) are accounted as
372 determining most of the variance of $\delta^{18}\text{O}$ attributable to geographical factors in the area. This
373 makes sense, since, from a physical point of view, elevation is a main determinant of
374 condensation temperature. The distance from coast controls moisture loss efficiency related to
375 sequential precipitation events on the course of the inland transport of the air parcel.

376 However, these factors do not fully account for second-order controls e.g. specific local air
377 mass trajectories, the differing seasonality of moisture sources for precipitation in Antarctica
378 (Sodemann and Stohl, 2009). By removing the driving effect of the geographical (first order)
379 factors with Eq. 3, the net effect of the previously mentioned second order factors (see section
380 2.3) was retained in the residuals. These ultimately provided the input values for the
381 variography and consequently the residual grid when the isoscape was modeled.

382

383 **4.2. Variography and isoscape derivation**

384 **4.2.1. Variography and kriging**

385 After the governing effect of geographical factors on firn/ice $\delta^{18}\text{O}$ variability had been
386 minimized, the dataset was prepared for variography. In contrast to mathematical
387 interpolation, where the same algorithm is applied to every location, geostatistical
388 interpolation using variograms is able to take regional properties into account (Herzfeld,
389 2004). It provides a spatially more data adaptive approach as underlined by Wang et al.
390 (2010) in his research on water stable isotopes.

391 The statistical uncertainty of the interpolation may come from variography: the nugget
392 ($\sqrt{C_0} = 0.36\text{‰}$) referring to the sampling error and the kriging standard deviation (KSD;
393 higher than 0.45‰ ; Fig. 4c) are governed by the spatial distribution of the ice cores (Chilès
394 and Delfiner, 2012). In an ideal case, exact interpolation is indicated by KSD being zero
395 (Wackernagel, 2003), which is anyhow unlikely in nature. If $C_0 > 0$, as in the present case (Fig.
396 4a), this was impossible. These uncertainties were acceptable, since the usual analytical
397 accuracy of the stable oxygen isotope analysis is $\sim 0.1\text{-}0.2\text{‰}$ depending on the applied isotope
398 analytical method (Lis et al., 2008). In addition, the well-known stratigraphic noise as a

399 natural factor in ice core records (Fisher et al., 1985) also affected the firm $\delta^{18}\text{O}$, causing
400 signal disturbance over small distances.

401

402 4.2.2. On isoscape and spatial range

403 The presented $\delta^{18}\text{O}$ isoscape describes an Antarctic macro region, 20% of which
404 ($\sim 0.5 \times 10^6 \text{ km}^2$) lies on ice shelves (Scambos et al., 2007). Oddly, it is not covered by the
405 continental $\delta^{18}\text{O}$ maps, despite the existence of data (Wang et al., 2009, 2010). As expected,
406 the mean stable isotope content indicated by the isoscape (Fig. 5) decreased with increasing
407 elevation & distance, and with temperatures decreasing inland. These phenomena can be
408 explained by isotopic fractionation inducing the preferential condensation of heavier
409 isotopologues during precipitation processes, leading to depleted water stable isotope
410 composition for both water vapor and precipitations penetrating the continent.

411 Ambient temperature is a primary physical factor in determining $\delta^{18}\text{O}$ variability in
412 precipitation and therefore also influences surface snow and consequently firm/ice isotope
413 variability. Thus, it was interesting to compare the spatial characteristics of $\delta^{18}\text{O}$ in surface
414 snow and temperature. Unfortunately, due to the lack of comparable direct instrumental
415 temperature measurements in space and time for such purposes, monthly mean near surface
416 (2 m) air temperature, representing the region of interest from 1970 to 1988 had to be used.
417 This data was extracted from NCEP/NCAR Reanalysis Products (Kalnay et al., 1996). The
418 same data treatment was applied for the temperature field as for the $\delta^{18}\text{O}$ records of the ice
419 cores, and variography was conducted on the residuals of its multiple regression model (Table
420 S3). The spatial range of the temperatures at the near surface- (2 m) was 428 km (Fig. 6).

421 It is well-known that the inversion and surface temperature are well correlated in
422 Antarctica (Jouzel et al., 1987), exhibiting a gradient of 0.67 for correspondent temperature
423 changes with changes at the surface being larger. Therefore, a positive correlation between
424 water isotope composition and surface temperature is expected.

425 A recent field study (Steen-Larsen et al., 2014) documented in the upper most 0.5 cm of
426 snow an imprint of the isotopic composition of vapor, by vapor exchange even between
427 precipitation events pointing to the imprint of ambient temperature variations via fractionation
428 processes. This surface processes can modify the temperature signal imprinted into the stable
429 water isotopes transported to the surface by precipitation from the cloud formation level. This
430 is further supported by the statistical evidence of related data (Hatvani and Kern, 2017). The
431 similar spatial variability domains for firn/ice $\delta^{18}\text{O}$ (350 km) and for the near surface
432 temperature (428 km) might be an indication that most of the observed water isotope
433 variations are temperature driven, yet the shorter domain for $\delta^{18}\text{O}$ calls for additional factors
434 to be involved.

435 Indeed, other phenomena, such as post deposition processes (e.g. stratigraphic noise
436 (Fisher et al., 1985)), can be also considered as major factors in the determination of $\delta^{18}\text{O}$
437 variability. It is interesting to note that a variogram analysis of surface snow accumulation in
438 an area overlapping with the domain of the present study reported the effective radii of spatial
439 autocorrelation to be 200-250 km from NE to SW and 100-150 km perpendicular to this
440 direction (Rotschky et al., 2007). The previously mentioned stratigraphic noise is therefore a
441 major factor in driving the spatial variability of snow accumulation.

442 Thus, the intermediate “position” of the firn/ice $\delta^{18}\text{O}$ spatial range between the ranges
443 characterizing the spatial variability of air temperature and snow accumulation reinforces the
444 notion that a combination of these processes is responsible for firn/ice $\delta^{18}\text{O}$ spatial variability.

445

446 4.2.3. A practical message for future site selection

447 If the aim is to study spatial (from regional to continental) variations of ice/firn stable
448 isotopes one or two drilling sites are unsatisfactory. Therefore, in the case of an array of ice
449 cores geostatistical planning is inevitable to optimize sampling, as done in the case of the
450 International Trans-Antarctic Scientific Expedition (Cressie, 1998). In the presented region of
451 Antarctica, the 350 km spatial range conveys the clear message that the current set of ice
452 cores does not cover the whole sector. The area outside the coverage of the cores (outside the
453 union of the range ellipses (Fig. 5)) is where new ice cores can contribute the most to the ice
454 core network as an additional geostatistical criterion for optimal site selection (Vance et al.,
455 2016). The drilling of additional cores would be helpful in the improvement of the description
456 of spatial variability, as has also been suggested by the IPICS (2006) initiative. If samples are
457 taken by interpolation in the areas outside the range ellipses' union, the interdependence
458 structure of firn/ice $\delta^{18}\text{O}$ variability remains undetectable, as samples there are already quasi-
459 independent (Chilès and Delfiner, 2012). Naturally, if new cores are drilled, it may be
460 presumed that the spatial autocorrelation structure of the dataset will change, and therefore
461 after any such campaign, a recalibration would be required.

462

463 5. Conclusions

464 Using the obtained dataset, the regional dependence of firn/ice $\delta^{18}\text{O}$ variability on
465 geographical factors was determined. It was shown that (i) in the study area $\delta^{18}\text{O}$ variance was
466 most precisely estimated - taking multicollinearity into account as well - by employing
467 longitude, elevation and the distance from the coast in a multivariate regression model.

468 Consequently, after correction for the effect of the geographic influence, the spatial
469 autocorrelation structure was revealed using variography, serving as the basis for isoscape
470 derivation employing kriging. The 350 km spatial range explicitly indicates the areas not as
471 yet covered by the currently available network of ice cores. Furthermore, the geostatistical
472 findings support the notion that the combination of the spatial variability of air temperature
473 and snow accumulation is likely to regulate firn/ice $\delta^{18}\text{O}$ spatial variability. These results
474 bring us closer to the accomplishment of one of the ultimate aims of research in this field, an
475 improved continental isoscape for Antarctica, since it has so far been neglected in global
476 isoscapes (Terzer et al., 2013; van der Veer et al., 2009).

477 Furthermore, we provide additional information about the spatial extent of a common
478 water stable isotope signal in Antarctica and offer guidance to experimenters on where to drill
479 additional cores in order to improve the overall representativeness of the shallow Antarctic
480 ice/firn core network. Moreover, the derived isoscape can be used as a benchmark in model
481 validation of isotope enabled GCMs in the case of scarce station based precipitation stable
482 isotope records over Antarctica.

483

484 **6. Acknowledgements**

485 We the authors would like to thank Paul Thatcher for his work on our English version
486 and say thanks for the stimulating discussion with Julien P. Nicolas from the Ohio State
487 University. The work of I.G. Hatvani was supported within the framework of TÁMOP 4.2.4.
488 A/1-11-1-2012-0001 „National Excellence Program – Elaborating and operating an inland
489 student and researcher personal support system”. The project was subsidized by the European
490 Union and co-financed by the European Social Fund. Special thanks to D. Divine, C.M.
491 Laluraj for providing access to their data and the researchers who archived their Antarctic ice

492 core derived stable isotope data in PANGAEA. The NCEP Reanalysis data was provided by
493 the NOAA/OAR/ESRL PSD, Boulder, Colorado, USA, from their website at
494 <http://www.esrl.noaa.gov/psd/>. We would also like to give thanks for the support of the MTA
495 “Lendület” program (LP2012-27/2012) and the János Bolyai Research Scholarship of the
496 Hungarian Academy of Sciences. This is contribution No. 39 of 2ka Palaeoclimate Research
497 Group.

498

499

References

500

- 501 Altnau, S., Schlosser, E., Isaksson, E., Divine, D., 2015. Climatic signals from 76 shallow firn
502 cores in Dronning Maud Land, East Antarctica. *The Cryosphere* 9, 925-944.
- 503 Araguás-Araguás, L., Froehlich, K., Rozanski, K., 2000. Deuterium and oxygen-18 isotope
504 composition of precipitation and atmospheric moisture. *Hydrological Processes* 14,
505 1341-1355.
- 506 Bowen, G.J., 2010. Isoscapes: Spatial Pattern in Isotopic Biogeochemistry. *Annual Review of*
507 *Earth and Planetary Sciences* 38, 161-187.
- 508 Bowen, G.J., Revenaugh, J., 2003. Interpolating the isotopic composition of modern meteoric
509 precipitation. *Water Resources Research* 39, 1299.
- 510 Bowen, G.J., Wilkinson, B., 2002. Spatial distribution of $\delta^{18}\text{O}$ in meteoric precipitation.
511 *Geology* 30, 315-318.
- 512 Chilès, J.-P., Delfiner, P., 2012. *Geostatistics*. Wiley, Canada.
- 513 Coplen, T.B., 1994. Reporting of stable hydrogen, carbon and oxygen isotopic abundances.
514 *Pure App. Chem.* 66, 273-276.
- 515 Cressie, N., 1990. The origins of kriging. *Math Geol* 22, 239-252.
- 516 Cressie, N., 1993. *Statistics for Spatial Data*. John Wiley & Sons, Inc.
- 517 Cressie, N., 1998. Transect-Spacing Design of Ice Cores on the Antarctic Continent. *The*
518 *Canadian Journal of Statistics* 26, 405-418.
- 519 Dansgaard, W., 1964. Stable isotopes in precipitation. *Tellus* 16, 436-468.
- 520 Divine, D.V., Isaksson, E., Kaczmarska, M., Godtliabsen, F., Oerter, H., Schlosser, E.,
521 Johnsen, S.J., van den Broeke, M., Wa, R.S.W.v.d., 2009. Tropical Pacific - High
522 Latitude SouthAtlantic Teleconnections as Seen in the $\delta^{18}\text{O}$ Variability in Antarctic
523 Coastal Ice Cores. *J. Geophys.Res.* 114, D11112.
- 524 Draper, N.R., Smith, H., 1981. *Applied regression analysis*. Wiley.
- 525 EPICA, M., 2004. Eight glacial cycles from an Antarctic ice core. *Nature* 429, 623-628.
- 526 EPICA, M., 2006. One-to-one coupling of glacial climate variability in Greenland and
527 Antarctica. *Nature* 444, 195-198.

- 528 Fernandoy, F., Meyer, H., Oerter, H., Wilhelms, F., Graf, W., Schwander, J., 2010. Temporal
529 and spatial variation of stable-isotope ratios and accumulation rates in the hinterland of
530 Neumayer station, East Antarctica. *Journal of Glaciology* 56, 673-687.
- 531 Fisher, D.A., Reeh, N., Clausen, H.B., 1985. Stratigraphic noise in time series derived from
532 ice cores. *Ann. Glaciol* 7, 76-83.
- 533 Füst, A., Geiger, J., 2010. Monitoring planning and evaluation using geostatistics, I.
534 Geostatistical support for verification sampling based on professional opinion. *Földtani*
535 *Közlöny* 140, 303-312.
- 536 Graf, W., Moser, H., Reinwarth, O., Kipfstuhl, J., Oerter, H., Minikin, A., Wagenbach, D.,
537 1994. Snow-accumulation rates and isotopic content (2H, 3H) of near-surface firn from
538 the Filchner-Ronne Ice Shelf, Antarctica. *Annals of Glaciology* 20, 121-128.
- 539 Graf, W., Reinwarth, O., Oerter, H., Mayer, C., Lambrecht, A., 1999. Surface accumulation
540 on Foundation Ice Stream, Antarctica. *Annals of Glaciology* 29, 23-28.
- 541 Hammer, C.U., 1989. Dating by Physical and Chemical Seasonal Variations and Reference
542 Horizons, in: Oeschger, H., C.C. Langway, J. (Eds.), *The Environmental Record in*
543 *Glaciers and Ice Sheets*. John Wiley & Sons Limited, pp. 99-121.
- 544 Hatvani, I.G., Kern, Z., 2017. Weighting alternatives for water stable isotopes: statistical
545 comparison between station- and firn/ice records. *Polish Polar Research*, 38 (2) DOI:
546 10.1515/popore-2017-0006 (in press)
- 547 Hatvani, I.G., Magyar, N., Zessner, M., Kovács, J., Blaschke, A.P., 2014. The Water
548 Framework Directive: Can more information be extracted from groundwater data? A
549 case study of Seewinkel, Burgenland, eastern Austria. *Hydrogeol J* 22, 779-794.
- 550 Herzfeld, U.C., 2004. *Atlas of Antarctica: Topographic Maps from Geostatistical Analysis of*
551 *Satellite Radar Altimeter Data : with 169 Figures*. Springer.
- 552 Hohn, M.E., 1999. *Geostatistics and Petroleum Geology* 2ed. Springer Science+Business
553 *Media Dordrecht, The Netherlands*.
- 554 IPICS, I.P.i.I.C.S.-. 2006. The IPICS 2k Array: a network of ice core climate and climate
555 forcing records for the last two millennia. *International Partnerships in Ice Coring*
556 *Sciences* p. 4.
- 557 Jones, P.D., Briffa, K.R., Osborn, T.J., Lough, J.M., van Ommen, T.D., Vinther, B.M.,
558 Luterbacher, J., Wahl, E.R., Zwiers, F.W., Mann, M.E., Schmidt, G.A., Ammann, C.M.,
559 Buckley, B.M., Cobb, K.M., Esper, J., Goosse, H., Graham, N., Jansen, E., Kiefer, T.,
560 Kull, C., Küttel, M., Mosley-Thompson, E., Overpeck, J.T., Riedwyl, N., Schulz, M.,
561 Tudhope, A.W., Villalba, R., Wanner, H., Wolff, E., Xoplaki, E., 2009. High-resolution
562 palaeoclimatology of the last millennium: a review of current status and future
563 prospects. *The Holocene* 19, 3-49.
- 564 Jouzel, J., 2013. A brief history of ice core science over the last 50 yr. *Clim. Past* 9, 2525-
565 2547.
- 566 Jouzel, J., Lorius, C., Petit J. R., Genthon, C., Barkov, N. I., Kotlyakov, V. M., Petrov, V. M.,
567 1987. Vostok ice core: a continuous isotope temperature record over the last climatic
568 cycle (160,000 years). *Nature* 329, 402-408.
- 569 Kalnay, E., Kanamitsu, M., Kistler, R., Collins, W., Deaven, D., Gandin, L., Iredell, M., Saha,
570 S., White, G., Woollen, J., Zhu, Y., Leetmaa, A., Reynolds, R., Chelliah, M., Ebisuzaki,
571 W., Higgins, W., Janowiak, J., Mo, K.C., Ropelewski, C., Wang, J., Jenne, R., Joseph,

- 572 D., 1996. The NCEP/NCAR 40-Year Reanalysis Project. *Bulletin of the American*
573 *Meteorological Society* 77, 437-471.
- 574 Kern, Z., Kohán, B., Leuenberger, M., 2014. Precipitation isoscape of high reliefs:
575 interpolation scheme designed and tested for monthly resolved precipitation oxygen
576 isotope records of an Alpine domain. *Atmos. Chem. Phys.* 14, 1897-1907.
- 577 Kuramoto, T., Goto-Azuma, K., Hirabayashi, M., Miyake, T.i., Motoyama, H., Dahl-Jensen,
578 D., Steffensen, J.P., 2011. Seasonal variations of snow chemistry at NEEM, Greenland.
579 *Annals of Glaciology* 52, 193-200.
- 580 Lachniet, M.S., Lawson, D.E., Stephen, H., Sloat, A.R., Patterson, W.P., 2016. Isoscapes of
581 $\delta^{18}\text{O}$ and $\delta^2\text{H}$ reveal climatic forcings on Alaska and Yukon precipitation. *Water*
582 *Resources Research* 52, 6575-6586.
- 583 Lis, G., Wassenaar, L.I., Hendry, M.J., 2008. High-Precision Laser Spectroscopy D/H and
584 $^{18}\text{O}/^{16}\text{O}$ Measurements of Microliter Natural Water Samples. *Analytical Chemistry* 80,
585 287-293.
- 586 Liu, H., Jezek, K.C., Li, B., 1999. Development of an Antarctic digital elevation model by
587 integrating cartographic and remotely sensed data: A geographic information system
588 based approach. *Journal of Geophysical Research: Solid Earth* 104, 23199-23213.
- 589 Lorius, C., Merlivat, L., 1977. Distribution of mean surface stable isotope values in East
590 Antarctica: Observed changes with depth in the coastal area. *International Association*
591 *of Hydrological Sciences Publication* 118, 127-137.
- 592 Masson-Delmotte, V., Hou, S., Ekaykin, A., Jouzel, J., Aristarain, A., Bernardo, R.T.,
593 Bromwich, D., Cattani, O., Delmotte, M., Falourd, S., Frezzotti, M., Gallée, H., Genoni,
594 L., Isaksson, E., Landais, A., Helsen, M.M., Hoffmann, G., Lopez, J., Morgan, V.,
595 Motoyama, H., Noone, D., Oerter, H., Petit, J.R., Royer, A., Uemura, R., Schmidt,
596 G.A., Schlosser, E., Simões, J.C., Steig, E.J., Stenni, B., Stievenard, M., van den
597 Broeke, M.R., van de Wal, R.S.W., van de Berg, W.J., Vimeux, F., White, J.W.C.,
598 2008. A review of Antarctic surface snow isotopic composition: observations,
599 atmospheric circulation, and isotopic modeling. *Journal of Climate* 21, 3359-3387.
- 600 Matheron, G., 1965. *Les Variables régionalisées et leur estimation: une application de la*
601 *théorie des fonctions aléatoires aux sciences de la nature.* Masson et Cie.
- 602 Merlivat, L., Jouzel, J., 1979. Global climatic interpretation of the deuterium-oxygen 18
603 relationship for precipitation. *Journal of Geophysical Research: Oceans* 84, 5029-5033.
- 604 Molnár, S., Füst, A., Szidarovszky, F., Molnár, M., 2010. Models in environmental
605 informatics II. Szent István University, Department of Informatics, Gödöllő, Hungary.
- 606 Naik, S.S., Thamban, M., Laluraj, C.M., Redkar, B.L., Chaturvedi, A., 2010. A century of
607 climate variability in central Dronning Maud Land, East Antarctica, and its relation to
608 Southern Annular Mode and El Niño-Southern Oscillation. *Journal of Geophysical*
609 *Research: Atmospheres* 115, D16102.
- 610 NGRIP, N.G.I.C.P.m., 2004. High-resolution record of Northern Hemisphere climate
611 extending into the last interglacial period. *Nature* 431, 147-151.
- 612 NOAA, 2014. p. Paleoclimatology database.
- 613 O'Brien, R.M., 2007. A Caution Regarding Rules of Thumb for Variance Inflation Factors.
614 *Quality & Quantity* 41, 673-690.

- 615 Oerter, H., Wilhelms, F., Jung-Rothenhäusler, F., Göktas, F., Miller, H., Graf, W., Sommer,
616 S., 2000. Accumulation rates in Dronning Maud Land, Antarctica, as revealed by
617 dielectric-profiling measurements of shallow firn cores. *Annals of Glaciology* 30, 27-
618 34.
- 619 Oliver, M.A., Webster, R., 2014. A tutorial guide to geostatistics: Computing and modelling
620 variograms and kriging. *CATENA* 113, 56-69.
- 621 PANGAEA, 2014. p. Paleoclimatology database.
- 622 Rotschky, G., Holmlund, P., Isaksson, E., Mulvaney, R., Oerter, H., Van den Broeke, M.R.,
623 Winther, J.-G., 2007. A new surface accumulation map for western Dronning Maud
624 Land, Antarctica, from interpolation of point measurements. *Journal of Glaciology* 53,
625 385-398.
- 626 Scambos, T.A., Haran, T.M., Fahnestock, M.A., Painter, T.H., Bohlander, J., 2007. MODIS-
627 based Mosaic of Antarctica (MOA) data sets: Continent-wide surface morphology and
628 snow grain size. *Remote Sensing of Environment* 111, 242-257.
- 629 Schlosser, E., Oerter, H., 2002. Shallow firn cones from Neumayer, Ekströmsisen, Antarctica: a
630 comparison of accumulation rates and stable-isotope ratios. *Annals of Glaciology* 35,
631 91-96.
- 632 Sjolte, J., Hoffmann, G., Johnsen, S.J., Vinther, B.M., Masson-Delmotte, V., Sturm, C., 2011.
633 Modeling the water isotopes in Greenland precipitation 1959–2001 with the meso-scale
634 model REMO-iso. *Journal of Geophysical Research: Atmospheres* 116, n/a-n/a.
- 635 Smith, B.T., Van Ommen, T.D., Morgan, V.I., 2002. Distribution of oxygen isotope ratios and
636 snow accumulation rates in Wilhelm II Land, East Antarctica. *Annals of Glaciology* 35,
637 107-110.
- 638 Sodemann, H., Stohl, A., 2009. Asymmetries in the moisture origin of Antarctic precipitation.
639 *Geophysical Research Letters* 36, L22803.
- 640 Steen-Larsen, H.C., Masson-Delmotte, V., Hirabayashi, M., Winkler, R., Satow, K., Prié, F.,
641 Bayou, N., Brun, E., Cuffey, K.M., Dahl-Jensen, D., Dumont, M., Guillevic, M.,
642 Kipfstuhl, S., Landais, A., Popp, T., Risi, C., Steffen, K., Stenni, B., Sveinbjörnsdóttir,
643 A.E., 2014. What controls the isotopic composition of Greenland surface snow? *Climate*
644 *of the Past* 10, 377-392.
- 645 Steig, E.J., Mayewski, P.A., Dixon, D.A., Kaspari, S.D., Frey, M.M., Schneider, D.P.,
646 Arcone, S.A., Hamilton, G.S., Spikes, V.B., Albert, M., Meese, D.A., Gow, A.J.,
647 Shuman, C.A., White, J.W.C., Sneed, S., Flaherty, J., Wumkes, M., 2005. High-
648 resolution ice cores from US ITASE (West Antarctica): development and validation of
649 chronologies and determination of precision and accuracy. *Annals of Glaciology* 41, 77-
650 84.
- 651 Sturm, K., Hoffmann, G., Langmann, B., Stichler, W., 2005. Simulation of $\delta^{18}\text{O}$ in
652 precipitation by the regional circulation model REMOiso. *Hydrological Processes* 19,
653 3425-3444.
- 654 Terzer, S., Wassenaar, L.I., Araguás-Araguás, L.J., Aggarwal, P.K., 2013. Global isoscapes
655 for $\delta^{18}\text{O}$ and $\delta^2\text{H}$ in precipitation: improved prediction using regionalized climatic
656 regression models. *Hydrol. Earth Syst. Sci.* 17, 4713-4728.

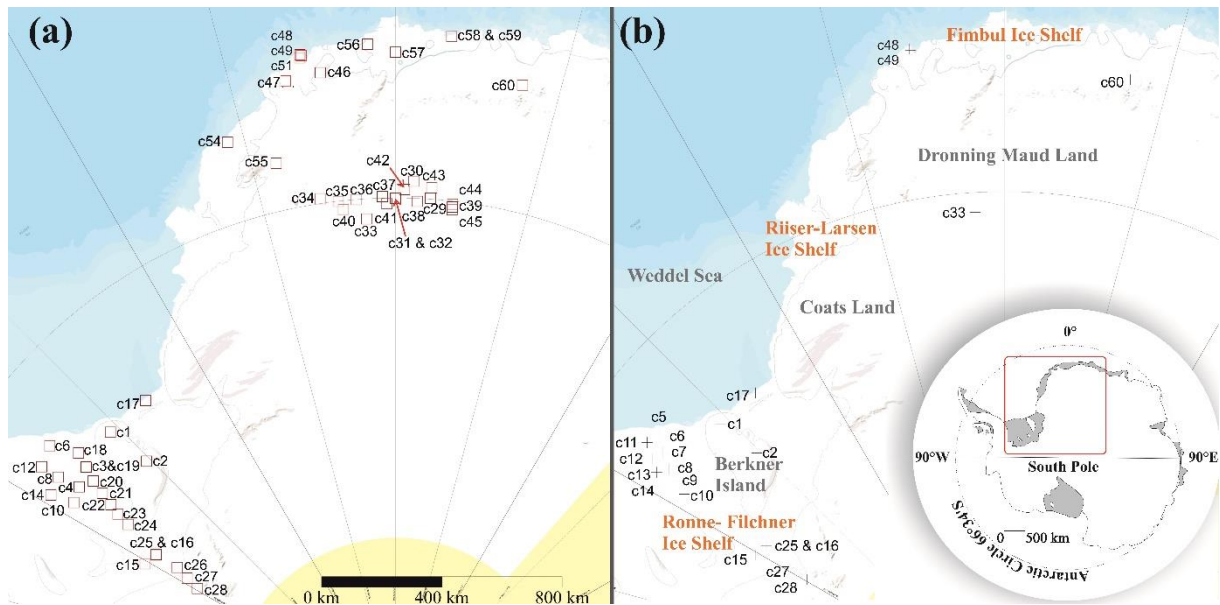
- 657 van der Veer, G., Voerkelius, S., Lorentz, G., Heiss, G., Hoogewerff, J.A., 2009. Spatial
658 interpolation of the deuterium and oxygen-18 composition of global precipitation using
659 temperature as ancillary variable. *Journal of Geochemical Exploration* 101, 175-184.
- 660 Vance, T.R., Roberts, J.L., Moy, A.D., Curran, M.A.J., Tozer, C.R., Gallant, A.J.E., Abram,
661 N.J., van Ommen, T.D., Young, D.A., Grima, C., Blankenship, D.D., Siegert, M.J.,
662 2016. Optimal site selection for a high-resolution ice core record in East Antarctica.
663 *Clim. Past* 12, 595-610.
- 664 Vaughan, D.G., Bamber, J.L., Giovinetto, M., Russell, J., Cooper, A.P.R., 1999.
665 Reassessment of Net Surface Mass Balance in Antarctica. *Journal of Climate* 12, 933-
666 946.
- 667 Wackernagel, H., 2003. *Multivariate Geostatistics*, 3 ed. Springer-Verlag Berlin Heidelberg.
- 668 Wang, Y., Hou, S., Masson-Delmotte, V., Jouzel, J., 2009. A new spatial distribution map of
669 $\delta^{18}\text{O}$ in Antarctic surface snow. *Geophysical Research Letters* 36, L06501.
- 670 Wang, Y., Hou, S., Masson-Delmotte, V., Jouzel, J., 2010. A generalized additive model for
671 the spatial distribution of stable isotopic composition in Antarctic surface snow.
672 *Chemical Geology* 271, 133-141.
- 673 Webster, R., Oliver, M.A., 2008. *Geostatistics for Environmental Scientists*, 2 ed. John Wiley
674 & Sons, Ltd.
- 675 Werner, M., Heimann, M., 2002. Modeling interannual variability of water isotopes in
676 Greenland and Antarctica. *Journal of Geophysical Research: Atmospheres* 107, ACL 1-
677 1-ACL 1-13.
- 678 Werner, M., Langebroek, P.M., Carlsen, T., Herold, M., Lohmann, G., 2011. Stable water
679 isotopes in the ECHAM5 general circulation model: Toward high-resolution isotope
680 modeling on a global scale. *Journal of Geophysical Research: Atmospheres* 116.
- 681 Wolff, E.W., Chappellaz, J., Blunier, T., Rasmussen, S.O., Svensson, A., 2010. Millennial-
682 scale variability during the last glacial: The ice core record. *Quaternary Science*
683 *Reviews* 29, 2828-2838.
- 684 Xi, X., 2014. A Review of Water Isotopes in Atmospheric General Circulation Models:
685 Recent Advances and Future Prospects. *International Journal of Atmospheric Sciences*
686 2014, 16.

687

688

689

Figure captions

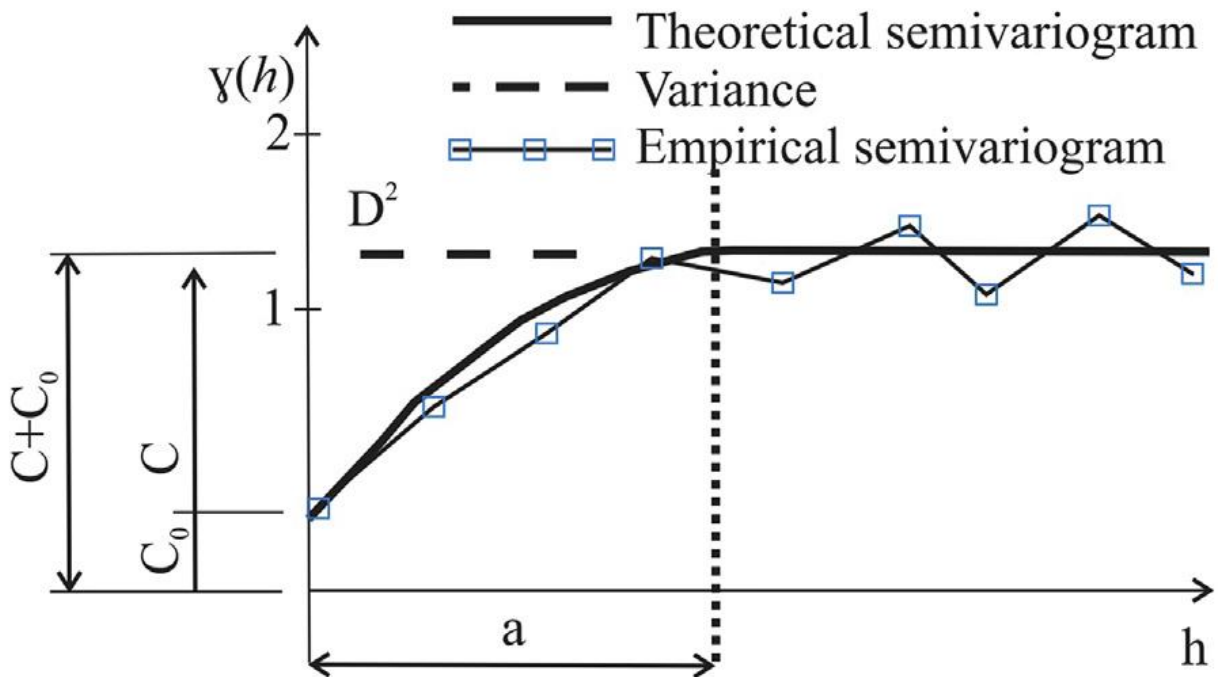


690

691 Fig. 1. Spatial distribution of the analyzed (a) $\delta^{18}\text{O}$ and (b) $\delta^2\text{H}$ ice core records. The study

692 area is marked by a red rectangle on the inset map (bottom right)

693

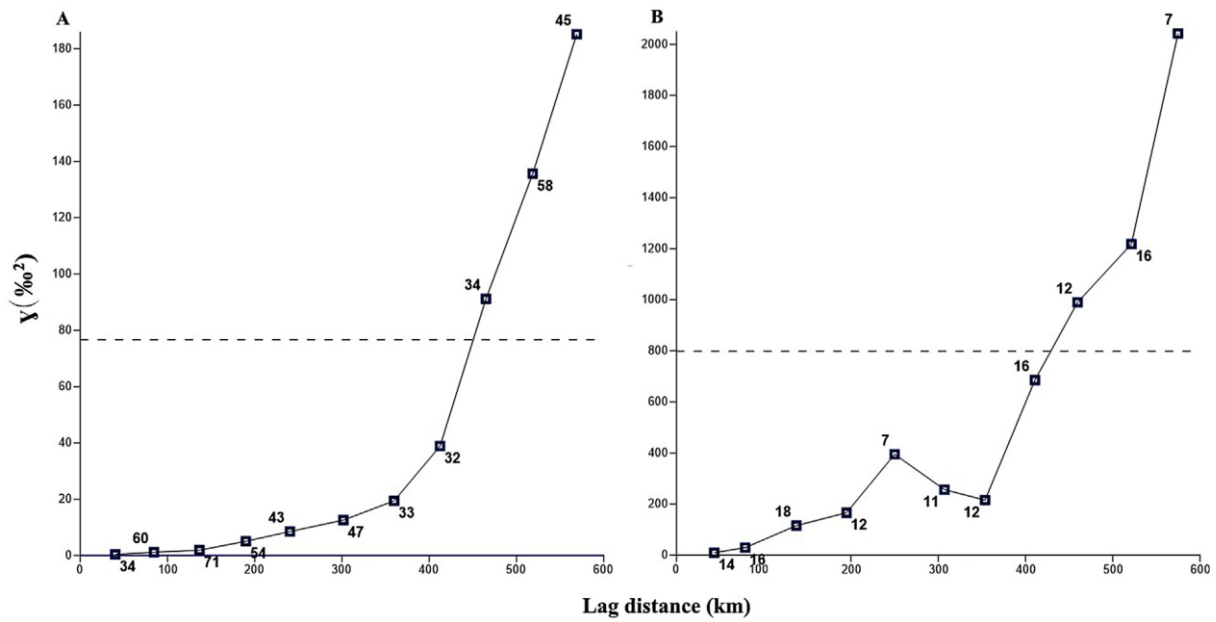


694

695 Fig. 2. Properties of the semivariogram, where “a” stands for the range, “C” for the reduced

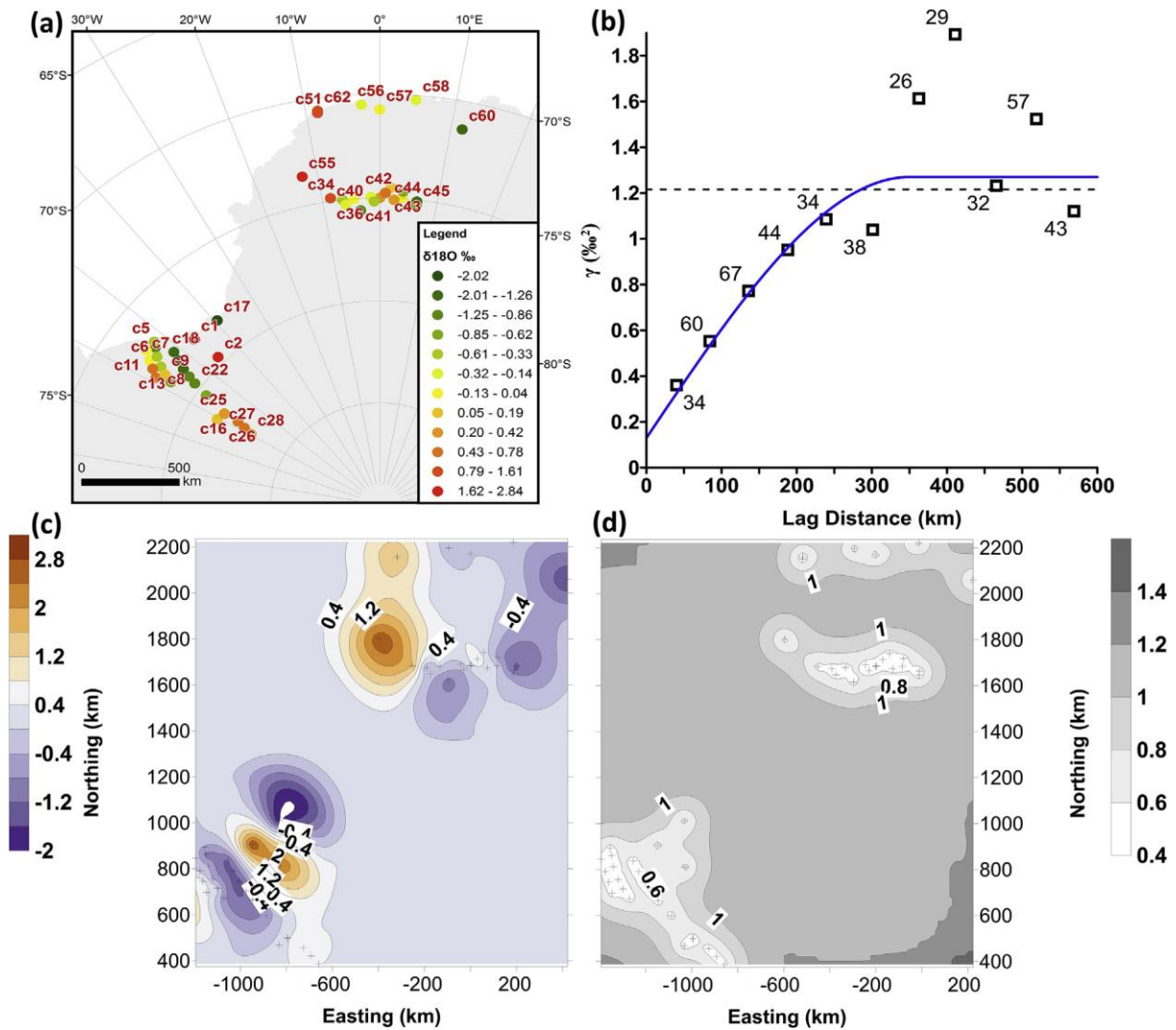
696 sill and “C₀” for the nugget, if C₀>0, “h” for lag distance, and “D²” for the variance of the

697 whole investigated data set; based on Füst and Geiger (2010)



698

699 Fig. 3. (a) Empirical semivariogram (squares) derived from the mean original and (1970-
700 1988) $\delta^{18}\text{O}$ and (b) (1970-1989) $\delta^2\text{H}$ values, with the broken line indicating the variance. The
701 numbers indicate the number of data pairs that were used to derive the variogram value for a
702 particular bin; bin widths were 55 km.



703

704

705

706

707

708

709

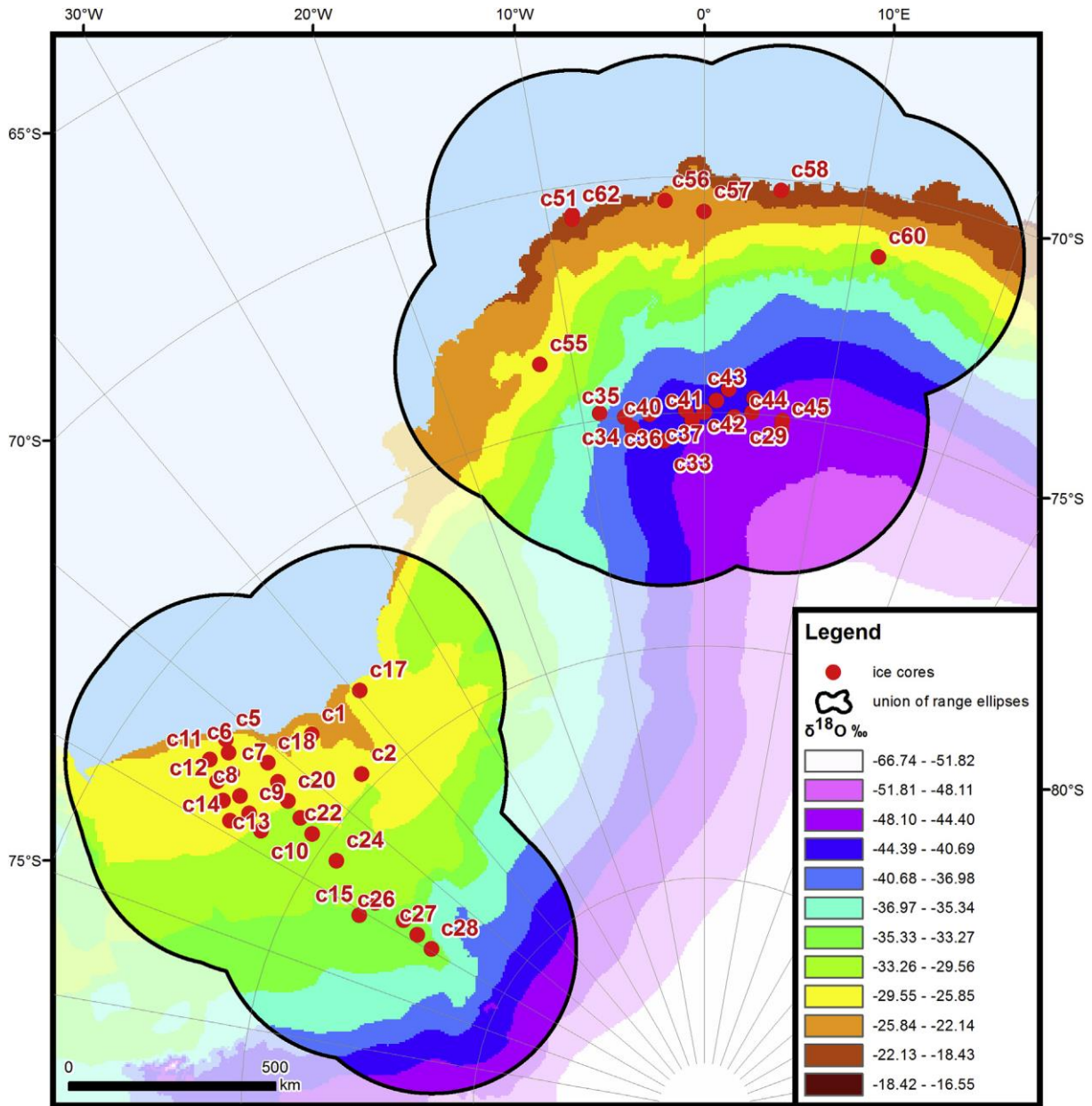
710

711

712

713

Fig. 4. Map of point residuals, variogram plot, and kriged map of the time average (1970-1988) $\delta^{18}\text{O}$ residuals and the standard deviation of kriging. (a) map of point residuals of the multiple regression; (b) empirical (blue squares) semivariogram and spherical theoretical model (blue line) ($C_0=0.13$; $C_0 + C=1.27$; $a=350$ km; $r^2=0.72$; bin width ~ 55 km) of the residuals. The variance is marked by the broken line. The numbers indicate the number of data pairs that were used to derive the variogram value (blue squares) for a particular bin in (b). (c) The ordinary point kriged map of the residuals; (d) the standard deviation of kriging. The faded crosses mark the locations of the ice cores in (c) & (d). Easting is the distance from the Prime Meridian, negative towards W and positive to E, while Northing is the distance from the South Pole, both in km.



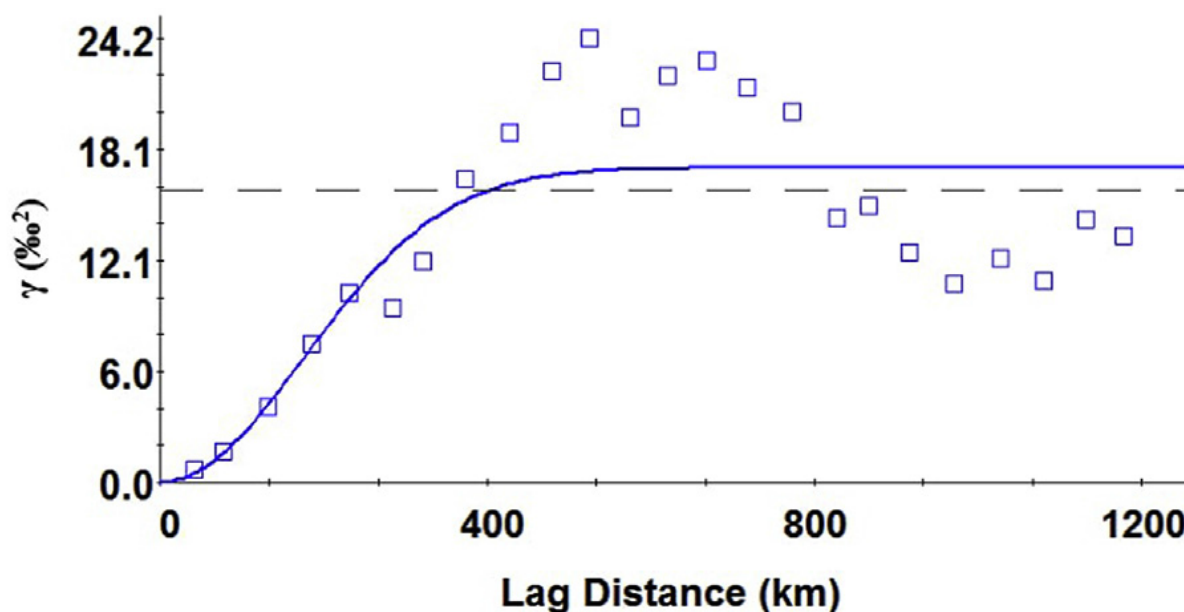
714

715 Fig. 5. Isoscape of $\delta^{18}\text{O}$ for the region for 1970-1988. The union of the 350km range ellipses

716 is marked with a black line. Isotropy was assumed, as the direction subsets proved

717 insufficient in the course of the exploration of anisotropy. Red dots mark the ice cores

718 used in the study.



719

720 Fig. 6. Empirical semivariogram of residual near surface (2m) temperature data (see Table S3)

721 for the region (1970-1988) marked with black squares and the fitted theoretical Gaussian

722 model (blue line)

723

724

Tables

725

726 **Table 1. Regression models of water stable isotopes using geographical variables in**

727 **Antarctica overlapping with the study area**

Study	Used independent variables	Estimated dependent variables	Scale
Masson-Delmotte et al., 2008	sin(LAT), ELE, D	$\delta^{18}\text{O}$, $\delta^2\text{H}$	Continental
Wang et al., 2010	LAT, LON, ELE, D	$\delta^{18}\text{O}$, $\delta^2\text{H}$	
Wang, 2009	$ \sin(\text{LAT}) ^2$, $ \sin(\text{LAT}) $, ELE	$\delta^{18}\text{O}$	
Altnau et al., 2015	ELE	$\delta^{18}\text{O}$	Regional
This study	LON, ELE, D	$\delta^{18}\text{O}$	

728